A Two-Dimensional Theory for Rotor Blade Flutter in Forward Flight

K. W. SHIPMAN* AND E. R. WOOD†
Rochester Applied Science Associates, Inc., Rochester, N. Y.

Presented is a theoretical method for determining rotor blade flutter in forward flight. The theory accounts for the unsteady aerodynamic contribution of the wake below the rotor. This is made possible due to certain simplifying assumptions of the authors regarding the rotor's wake at the onset of flutter. In particular, it is assumed at the onset of flutter that oscillations begin to build up prior to the blade reaching a critical azimuth position, then decay as the blade moves beyond this point. Based upon this a wake model is postulated and the theory developed. The resulting lift deficiency function is compared with that of Loewy[1] and Theodorsen.[2] It is shown in limiting cases that the work presented is consistent with earlier flutter theory. The theory is applied to bending-torsion flutter for the tip segment of a rotor blade. Here, beyond a certain value of advance ratio, the influence of advance ratio on flutter speed is found to be essentially constant.

Nomenclature‡

a	= nondimensional elastic axis location, measured from midchord
b	= number of blades
c	= semichord length, in.
$C(k)$	= Theodorsen's lift deficiency function
$C'(k,m,\hat{h})$	= Loewy's lift deficiency function
$C_1(k,\mu,\lambda)$	= present lift deficiency function
c.g.	= center of gravity
e.a.	= elastic axis
$f(\xi_0)$	= decay function centered about $\xi_0 = 0$
$\Delta F_1, \Delta F_2, \Delta F_3, \Delta F_4, \Delta F_5$	= terms arising due to the decay function; see Eqs. (23–25) and Eq. (35)
g	= damping coefficient
h_0	= amplitude of deflection ($h = h_0 e^{i\omega t}$)
h	= nondimensional vertical deflection (positive downward)
$\hat{h}$	= nondimensional wake spacing, $\lambda 2\pi R/bc$
$H_n^{(2)}(k)$	= Hankel function of the second kind and order n
I_α	= mass moment of inertia about the elastic axis, lb in.^{2}/in.
k	= reduced frequency ($\omega c/V$)
L	= lift, lb/in. [Eq. (28)]
L_A	= rotation coefficient for lift [Eq. (30)]
L_H	= deflection coefficient for lift [Eq. (29)]
m	= mass distribution, lb/in.; also, frequency ratio = ω/Ω (Loewy)
M_{ea}	= aerodynamic moment about the elastic axis, in.-lb/in.
M_A	= rotation coefficient for moment [Eq. (33)]
M_H	= deflection coefficient for moment [Eq. (32)]
$\hat{p}$	= growth and decay rate
p	= pressure, psi
Δp	= pressure difference across the airfoil, psi
R	= blade radius, in. or ft
s and s_1	= nondimensional horizontal distances
t	= time, sec
U	= total velocity ($\Omega R + V$), in./sec
v_a	= downwash along the airfoil, in./sec
v_i	= induced velocity, in./sec
V	= forward flight velocity, in./sec or knots
$W(k\hat{h},m)$	= Loewy's weighting function due to shed wakes
$W(k,s,\hat{h})$	= present weighting function due to shed wakes
ΔW	= segment of present weighting function due to decay
x	= nondimensional distance from midchord along the airfoil
$x_{c.g.}$	= nondimensional c.g. location, percent chord
Z	= frequency-damping variable [Eq. (39)]
α	= airfoil rotation
α_0	= amplitude of rotation ($\alpha = \alpha_0 e^{i\omega t}$)
γ_a	= incremental bound vorticity strength, in./sec
γ_n	= shed vorticity strength, in./sec ($n = 0,1,2, \ldots$)
Γ_a	= total bound vorticity, in.^{2}/sec
$\bar{\Gamma}_a$	= bound vorticity factor, $\left(e^{ik}\int_{-1}^{1}\bar{\gamma}_a(x)dx\right)$
ϕ	= phase angle
Φ	= velocity potential
κ	= inverse mass ratio ($\pi\rho c^2/m$)
λ	= inflow ratio, $v_i/\Omega R$
μ	= advance ratio, $V/\Omega R$
ρ	= air density, lb sec^2/in.^{4}
$\Delta\psi_{FL}$	= complement of the azimuth angle at which the blade tip reaches flutter speed
ξ	= nondimensional horizontal distance from the midchord
ω	= flutter frequency, rad/sec
ω_h	= natural bending frequency
ω_α	= natural torsional frequency
Ω	= rotor speed, rpm or rad/sec

Subscripts

FL	= flutter
L	= lower
U	= upper
t	= tangential
0,1, . . . , n	= wake number

Superscript

—	= denotes independence from time

Received October 13, 1970; revision received June 28, 1971; presented at the 26th Annual National Forum of the American Helicopter Society, June 1970. This work was done while both authors were at the Georgia Institute of Technology, Atlanta, Ga.

Index categories: Rotary Wing and VTOL Aerodynamics; Aeroelasticity and Hydroelasticity; VTOL Structural Design (Including Loads).

* Research Engineer. Associate Member AIAA.

† Assistant Director of Engineering. Associate Fellow AIAA.

‡ Distances have been nondimensionalized by the semichord length, c.

Introduction

THIS paper is directed at improving forward flight blade flutter analysis. The method presented is based upon extending Loewy's[1] theory for a hovering rotor to forward flight. If the magnitude of rotor downwash velocities is such that wakes shed from preceding blades remain relatively

near the rotor disk, then neither quasi-steady nor fixed-wing unsteady aerodynamics can be reliably used for predicting blade flutter. This influence of the layers of shed vorticity was accounted for by Loewy[1] in 1957 in his flutter theory for a hovering rotor. He considered a two-dimensional wake model. His results were valid so long as the flow could be considered essentially incompressible,§ and so long as rotor induced velocities were such that wakes shed from the rotor could be considered a series of horizontal sheets. We note that for high inflows the form of the wake helix would be such that this approximation would not be valid: However, for this condition the wake is removed from the rotor and the contribution of the wake to the unsteady aerodynamics becomes less significant.

Several interesting results could be noted from Loewy's theory. First, if we let the wake spacing become infinite, then this theory, as might be expected, reduces to that of Theodorsen[2] for the fixed wing case. Second, the effect of reducing the spacing of the wake layers, thus bringing them closer to the rotor, was destabilizing. That is, the most critical flutter condition appeared to be at very low inflow values.

Given in this paper is a method which accounts for the unsteady contribution of a simplified wake model for the forward flight condition. Currently to meet forward flight blade flutter requirements the rotorcraft manufacturer must rely on: 1) quasi-fixed wing blade flutter analysis, which does not account for the unsteady contribution of the wake below the rotor; and 2) rotor whirl tests at normal and overspeed conditions which, while providing information in regard to blade flutter, do not accurately simulate either blade dynamics or unsteady aerodynamics in forward flight. Accounting for the contribution of the rotor's wake in forward flight could be especially important for the case of a compound helicopter. Here, in high-speed flight the rotor may be partially or fully unloaded and set at zero angle-of-attack. This would result in wakes near the rotor due to very low or zero induced flow with no downwash contribution from the forward flight velocity component.

Extension of the work of Theodorsen[2] and Loewy[1] to forward flight for a rotor blade (in the general case) presents a formidable mathematical problem. Here, the effect of a shed skewed helical wake would have to be considered and the contribution of each element of that wake on each segment of the blade at each azimuth position accounted for. However, closer examination of this problem reveals that it is possible to make several rational assumptions that make the problem tractable. A description of the mathematical model, its formulation, and the results which are obtained are the subject of this paper and are presented in the paragraphs to follow.

Background

In 1935 Theodorsen[2] considered a wing oscillating in simple harmonic motion and treated the resulting shed vorticity, which was sinusoidal and of constant amplitude. For a wing oscillating at frequency ω the unsteady lift was given by

$$L = \pi\rho\omega^2c^3\{L_h h_0/c + [L_\alpha - (\tfrac{1}{2} + a)L_h]\alpha_0\} \qquad (1)$$

where c is the semichord length and

$$L_h = 1 - 2iC(k)/k$$

and

$$L_\alpha = \tfrac{1}{2} - 2i[\tfrac{1}{2} + (1 - i/k)C(k)]/k$$

Theodorsen's well-known lift deficiency function, $C(k)$, could be expressed in the form

$$C(k) = H_1^{(2)}(k)/[H_1^{(2)}(k) + iH_0^{(2)}(k)] \qquad (2)$$

where $H_n^{(2)}(k)$ represent Hankel functions of the second kind, and where the reduced frequency, k, is defined as $k \equiv \omega c/V$.

The lift relation of Eq. (1) was confirmed by Schwarz[3] in 1940. Schwarz applied Söhngen's[4] inversion formula and was able to determine the vorticity, and hence the pressure distribution and lift on an airfoil in terms of general motion. This concept was later extended by W. P. Jones[5] who allowed the strength of the airfoil's motion to grow or decay exponentially. This meant that the amplitude of motion could be written

$$A = \bar{A}e^{\hat{p}t}e^{i\omega t}$$

where for $\hat{p}$ positive, the motion would grow with time. For decaying motion $\hat{p}$ would be negative. As the buildup or decay rate $\hat{p}$ approached zero through positive values, Jones' lift deficiency function approached that of Theodorsen.

J. P. Jones[8] postulated that increases in vibratory stresses noted by J. R. Meyer[9] in hover tests of a model rotor blade were due to wake effects. He developed a two-dimensional theory to take into account the wake and obtained good qualitative agreement with the previous experimental results. Loewy[1] obtained a lift deficiency function for finding the flutter boundary for a hovering rotor. He accounted for vortex sheets below the blade which had been shed by previous blade passes. With a vibratory frequency ω and a blade rotational frequency of Ω, Loewy's lift deficiency function was given by

$$C'(k,m,\hat{h}) = \frac{H_1^{(2)}(k) + 2J_1(k)W(k\hat{h},m)}{H_1^{(2)}(k) + iH_0^{(2)}(k) + 2W(k\hat{h},m)[J_1(k) + iJ_0(k)]} \qquad (3)$$

where the effect of the wakes shed below the plane of the rotor appears in the weighting function

$$W(k\hat{h},m) = 1/(e^{k\hat{h}}e^{i2\pi m/b} - 1) \qquad (4)$$

in which m, b, and $\hat{h}$ represent frequency ratio, number of blades, and wake spacing, respectively, as defined in the notation.

This paper builds upon the previous work to the following extent. A wake model for forward flight is postulated by the authors. The fundamental approach to the flutter problem is that of Theodorsen.[2] The analytical method followed is that of Schwarz.[3] The flutter wake model is an extension to forward flight of the model treated by Loewy,[1] with the exception that segments of vorticity build-up and decay in the manner of those treated by Jones.[5]

Theoretical Analysis

Method of Approach

Consider a rotary-wing aircraft in steady-state level flight. We examine the unsteady aerodynamics acting on an advancing blade (Fig. 4).

The basic assumptions incorporated are as follows: 1) two-dimensional, incompressible potential flow. 2) Respective layers of the wake are two-dimensionalized and treated as parallel horizontal sheets. 3) In forward flight, each blade of the rotor will respond in the same manner as every other blade. 4) The most critical azimuth positions of the blade in forward flight for the onset of flutter are near $\psi = 90°$ and $\psi = 270°$. This paper is concerned with the 90°-azimuth position, but extension of this work to the 270°-case is straightforward. 5) At the onset of blade flutter oscillations will begin to build up prior to the blade reaching the critical azimuth position, and these oscillations will decay as the blade moves beyond the critical azimuth position.

§ Extension of Loewy's theory to include compressibility effects has been recently considered by Jones[6] and by Hammond.[7]

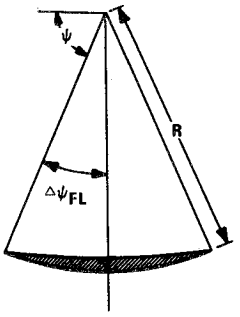

Fig. 1 Unstable region encountered by advancing blade.

At a specified radial location r on the blade, the local tangential velocity would be given by

$$U_t(r) = \Omega r + V \sin\psi$$

If we assume that the flutter speed for this blade segment is such that $U_{FL}(r) < \Omega r + V$ then, during each blade revolution the blade segment at r will experience velocities which will increase to the flutter speed and beyond, then return through the flutter boundary to lower airspeeds.

Extending this concept to both blade azimuth position and radial station, we observe that the blade tangential velocity at a given radial position will exceed the flutter speed in some region of rotor azimuth position if $V \sin\psi > U_{FL}(r) - \Omega r$. An example of this region is shown in Fig. 1.

We note that all points within the shaded region of Fig. 1 will experience negative damping. This negative damping will tend to cause blade motion to grow. We also observe that in the region $\psi \leq \pi/2 - \Delta\psi_{FL}$ the damping will decrease as ψ approaches $(\pi/2 - \Delta\psi_{FL})$, whereas in the region $\psi \geq \pi/2 + \Delta\psi_{FL}$, damping will be positive and will increase so that a blade instability would tend to die out.

Consider the effect of this variation in damping on an outboard portion of the advancing blade. We would expect that as damping decreased with the blade approaching $\psi = 90°$, the amplitude of oscillations would build up. Conversely, as the blade advanced beyond the $\psi = 90°$ position, damping would increase and there would be a corresponding decrease in blade vibratory amplitude. This build-up and decay of blade amplitude would result in a distribution of shed vorticity as shown by Fig. 2. Here, we observe that timewise variations in amplitude of blade vibrations have resulted in spacewise variations in shed vorticity. Since we have assumed steady-state flight, similar segments of vorticity would be shed by each blade for each revolution. These vortex segments constitute the wake that will be treated in this analysis (see Fig. 4).

Based on the foregoing, the bound vorticity on the airfoil can be expressed as the product of a function of chordwise position, a decay function, and a harmonic function of time. We write the incremental bound vorticity as $\gamma_a = \bar{\gamma}_a(x) f(\xi_0) e^{i(\omega t + \phi)}$ where $f(\xi_0)$ is an assumed decay function centered about $\xi_0 = 0$. The limiting case of constant-strength shed vorticity, such as considered by Theodorsen[2] and Loewy[1] for their analyses, is simply achieved by taking $f(\xi_0) = 1$.

When the inflow velocity through the rotor is small, the shed vorticity remains close to the rotor and the wakes shed from each blade during several previous passes as well as the present pass must be considered. The build-up and decay of vorticity occurs within a double azimuth angle on either side of $\psi = 90°$. This region of the wake is indicated by

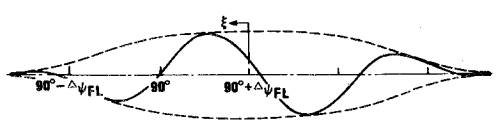

Fig. 2 Distribution of shed vorticity in unstable region.

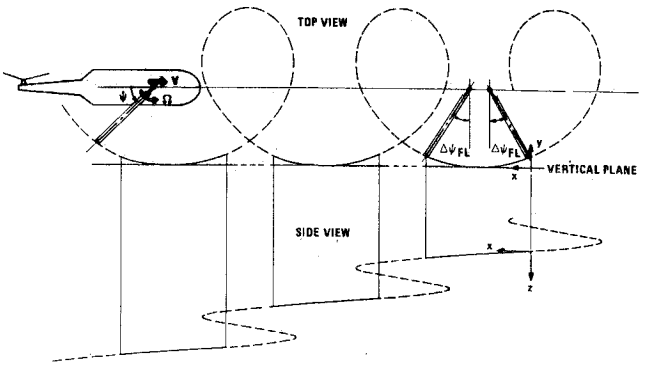

Fig. 3 Development of skewed helical wake.

the solid lines of Fig. 3. In this region the azimuth angle between a shed vortex filament and the reference blade may be ignored. The tip does not move very far from the vertical plane shown in Fig. 3 and so its path may be taken to lie in this plane.

Combining the vorticity segments given in Fig. 2, the resulting wake pattern is shown in Fig. 4. With the mathematical model defined, the problem now is to determine the pressure difference across the airfoil due to the vorticity shed in the wakes, and consequently to determine the unsteady lift and moment acting on the airfoil.

Analytical Development

The downwash which is induced by an element of vorticity located a distance cs_1 behind and $c\hat{h}$ below the point of interest is found from the Biot-Savart Law which states that

$$dv_a(x,t) = \gamma_n(s_1,t) s_1 ds_1 / 2\pi(s_1^2 + \hat{h}^2) \tag{5}$$

From Fig. 4 it can be seen that for a point at a distance xc behind the midchord on a blade, which is a distance Ut from the origin of the reference wake,

$$s_1 = \xi_n + ns + Ut/c - x$$

and

$$\hat{h} = \lambda 2\pi R/bc$$

where

$$s = \mu 2\pi R/bc$$

and ξ_n is the distance between the center of the nth wake and the location of the element of vorticity γ_n.

Integrating over the airfoil, the reference wake, and all of the previously shed wakes yields the downwash $v_a(x,t)$ which is

$$2\pi v_a(x,t) = \int_{-1}^{1} \frac{\gamma_a(\xi,t)d\xi}{\xi - x} + \int_{1}^{\infty} \frac{\gamma_0(\xi,t)d\xi}{\xi - x} + \sum_{n=1}^{\infty} \int_{-\infty}^{\infty} \frac{\gamma_n(\xi_n,t)(\xi_n + ns + Ut/c - x)}{(\xi_n + ns + Ut/c - x)^2 + n^2\hat{h}^2} d\xi_n \tag{6}$$

If the incremental bound vorticity is a harmonic function of time then it can be separated as

$$\gamma_a(x,t) = \bar{\gamma}_a(x) f(\xi_0) e^{i(\omega t + \phi)} \tag{7}$$

where $f(\xi_0)$ is some decay function centered about $\xi_0 = 0$. The vorticity shed at the trailing edge is

$$\gamma_0(1,t)d\xi = -(d\Gamma_a/dt)dt \tag{8}$$

Since

$$\Gamma_a = c \int_{-1}^{1} \gamma_a(x,t)dx$$

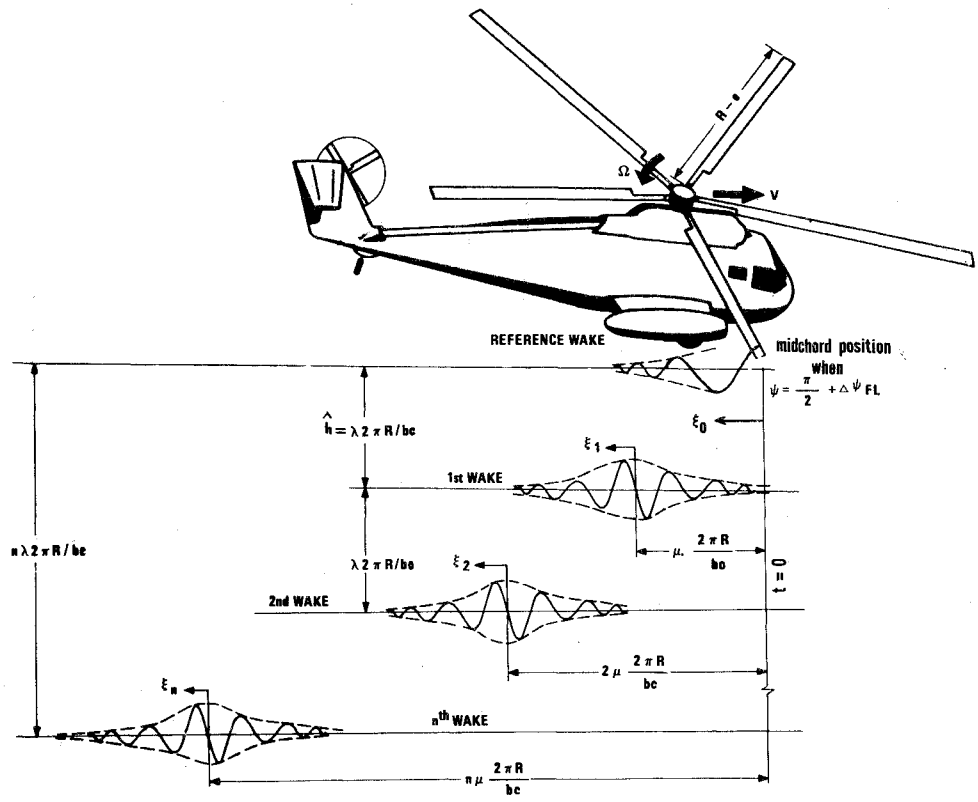

Fig. 4 Two-dimensional wake model for forward flight.

it is apparent from the definition in Eq. (7) that

$$\frac{\partial \Gamma_a}{\partial t} = c\left[i\omega f(\xi_0) + \frac{df}{d\xi_0}\frac{d\xi_0}{dt}\right]e^{i(\omega t+\phi)}\int_{-1}^{1}\bar{\gamma}_a(x)dx \quad (9)$$

But

$$\xi_0 = \xi - Ut/c$$

and

$$d\xi/dt = U/c$$

and so substituting Eq. (9) into Eq. (8) yields

$$\gamma_0(1,t) = -ik\bar{\Gamma}_a\left[f(\xi_0) - \frac{1}{ik}\frac{df}{d\xi_0}\right]e^{i(\omega t+\phi-k)} \quad (10)$$

where

$$\bar{\Gamma}_a = e^{ik}\int_{-1}^{1}\bar{\gamma}_a(x)dx$$

and

$$k = \omega c/\Omega R + V = \omega c/U \quad (11)$$

Since

$$\gamma_0(1,t - \Delta t) = \gamma_0(\xi,t)$$

where

$$U\Delta t/c = \xi - 1 = \xi_0 + Ut/c - 1$$

in which ξ refers to blade midchord in any position and ξ_0 refers to midchord when $\psi = \pi/2 + \Delta\psi_{FL}$, Eq. 10 can be written as

$$\gamma_0(\xi_0,t) = -ik\bar{\Gamma}_a\left[f(\xi_0) - \frac{1}{ik}\frac{df}{d\xi_0}\right]e^{i(\phi-k\xi_0)} \quad (12)$$

Since the vorticity distribution with respect to the center of each wake is the same for all wakes,

$$\gamma_n(\xi_n,t) = -ik\bar{\Gamma}_a\left[f(\xi_n) - \frac{1}{ik}\frac{df}{d\xi_n}\right]e^{i(\phi-k\xi_n)} \quad (13)$$

With the downwash on the blade given as

$$v_a(x,t) = \bar{v}_a(x)f(\xi_0)e^{i(\omega t+\phi)}$$

substitution of Eqs. (12) and (13) into Eq. (6) yields

$$2\pi\bar{v}_a(x) = \int_{-1}^{1}\frac{\bar{\gamma}_a(\xi)d\xi}{\xi - x} - ik\bar{\Gamma}_a \times \int_{1}^{\infty}\frac{[f(\xi_0) - (1/ik)(df/d\xi_0)]e^{-ik\xi_0}}{\xi_0 - x}d\xi_0 - \pi k\bar{\Gamma}_a e^{-ikx}[W(k,s,\hat{h}) + \Delta W] \quad (14)$$

where

$$W(k,s,\hat{h}) = 1/(e^{k\hat{h}}e^{-iks} - 1)$$

and

$$-i\pi\Delta W = \sum_{n=1}^{\infty}e^{ikns}\int_{-\infty}^{\infty}\left[f(n\hat{h}y - ns) - 1 - \frac{1}{ik}\frac{df}{d\xi_n}\right]\times \frac{ye^{-ikn\hat{h}y}}{y^2+1}dy \quad (15)$$

and where $n\hat{h}y = \xi_n + ns - x$ is the coordinate change used for the integrals in the summation in Eq. (6).

Pressure Equation

Using Söhngen's[4] inversion formula on Eq. (14) gives the incremental bound vorticity in terms of the downwash on the airfoil so that

$$\bar{\gamma}_a(x) = \frac{2}{\pi}\left(\frac{1-x}{1+x}\right)^{1/2}\times \left\{\int_{-1}^{1}\left(\frac{1+\xi}{1-\xi}\right)^{1/2}\frac{\bar{v}_a(\xi)}{x-\xi}d\xi + \frac{ik\bar{\Gamma}_a}{2\pi}\times \int_{-1}^{1}\left(\frac{1+\xi}{1-\xi}\right)^{1/2}\int_{1}^{\infty}\left[f(y) - \frac{1}{ik}\frac{df}{dy}\right]\frac{e^{-iky}}{y-\xi}dyd\xi + \tfrac{1}{2}k\bar{\Gamma}_a(W + \Delta W)\int_{-1}^{1}\left(\frac{1}{x-\xi}\right)^{1/2}\frac{e^{-ik\xi}}{x-\xi}d\xi\right\} \quad (16)$$

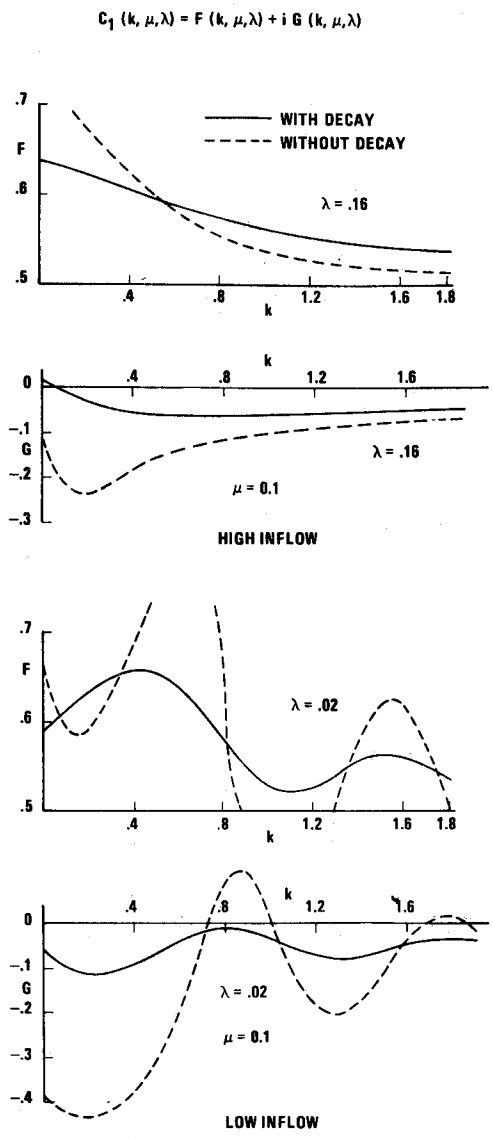

Fig. 5 Lift deficiency function for high and low inflow.

By integrating Eq. (16) over the chord, the total bound vorticity is found to be

$$\bar{\Gamma}_a = \frac{2\int_{-1}^{1}[(1+\xi/1-\xi)]^{1/2}\bar{v}_a(\xi)d\xi}{i\pi k\{\frac{1}{2}[H_1^{(2)}+iH_0^{(2)}]+\frac{1}{2}\Delta F_3+(W+\Delta W)(J_1+iJ_0)\}} \quad (17)$$

Bernoulli's pressure equation for unsteady motion,

$$\partial\Phi/\partial t + U/c(\partial\Phi/\partial x) + p/\rho = f(t)$$

and the relation between the velocity potential and the bound vorticity,

$$\Phi_U - \Phi_L = \int_{-1}^{x}\gamma_a(\xi,t)d\xi$$

can be combined to give

$$-\frac{\Delta p}{\rho} = U\gamma_a(x,t) + \int_{-1}^{x}\frac{\partial}{\partial t}\gamma_a(\xi,t)d\xi \quad (18)$$

With the pressure given as

$$\Delta p = \Delta\bar{p}(x)f(\xi_0)e^{i(\omega t+\phi)}$$

Eq. (16) becomes

$$\frac{-\Delta\bar{p}(x)}{\rho U} = \bar{\gamma}_a(x) + ik\int_{-1}^{x}\bar{\gamma}_a(\xi)d\xi \quad (19)$$

Substituting Eq. (16) into Eq. (19) and performing the necessary operations shows the unsteady pressure distribution to be

$$-\frac{\Delta\bar{p}(x)}{\rho U} = \frac{2}{\pi}\int_{-1}^{1}\left[\left(\frac{1-x}{1+x}\right)^{1/2}\left(\frac{1+\xi}{1-\xi}\right)^{1/2}\times\frac{1}{x-\xi} - ik\Omega_1(x,\xi)\right]\bar{v}_a(\xi)d\xi + \frac{2}{\pi}\times\frac{iH_0^{(2)}+\Delta F_1+2i(W+\Delta W)J_0}{H_1^{(2)}+iH_0^{(2)}+\Delta F_3+2(W+\Delta W)(J_1+iJ_0)}\times\left(\frac{1-x}{1+x}\right)^{1/2}\int_{-1}^{1}\left(\frac{1+\xi}{1-\xi}\right)^{1/2}\bar{v}_a(\xi)d\xi + \frac{2}{\pi}\times\frac{F_1(k,x)}{H_1^{(2)}+iH_0^{(2)}+\Delta F_3+2(W+\Delta W)(J_1+iJ_0)}\times\int_{-1}^{1}\left(\frac{1+\xi}{1-\xi}\right)^{1/2}\bar{v}_a(\xi)d\xi \quad (20)$$

where $F_1(k,x)$ is an integral along the reference wake involving the first and second derivatives of the decay function.

Lift Deficiency Function

Integrating Eq. (20) over the chord, the lift in terms of the downwash along the airfoil becomes

$$\frac{L}{2\rho Uc} = ik\int_{-1}^{1}(1-x^2)^{1/2}\bar{v}_a(x)dx + C_1(k,\mu,\lambda)\int_{-1}^{1}\left(\frac{1+x}{1-x}\right)^{1/2}\bar{v}_a(x)dx \quad (21)$$

where the lift deficiency function for a helicopter in forward flight is

$$C_1(k,\mu,\lambda) = \frac{H_1^{(2)}(k)+\Delta F_2(k)+2J_1(k)[W(k,s,\hat{h})+\Delta W]+\Delta F_4(k)}{H_1^{(2)}(k)+iH_0^{(2)}(k)+\Delta F_3(k)+2[W(k,s,\hat{h})+\Delta W][J_1(k)+iJ_0(k)]} \quad (22)$$

where

$$W(k,s,\hat{h}) = 1/(e^{k\hat{h}}e^{-iks}-1)$$
$$s = \mu 2\pi R/bc$$
$$\hat{h} = \lambda 2\pi R/bc$$

and where ΔW, $\Delta F_1(k)$, $\Delta F_2(k)$, $\Delta F_3(k)$, and $\Delta F_4(k)$ are the terms added to account for the buildup and decay of the strength of shed vorticity. These terms are the integrals

$$\Delta F_1 = \Delta F_3 - \Delta F_2$$

$$\Delta F_2 = -\frac{2}{\pi}\int_1^{\infty}\left[f(y) - 1 - \frac{1}{ik}\frac{df}{dk}\right]\frac{ye^{-iky}}{(y^2-1)^{1/2}}dy \quad (23)$$

$$\Delta F_3 = -\frac{2}{\pi}\int_1^{\infty}\left[f(y) - 1 - \frac{1}{ik}\frac{df}{dy}\right]\left(\frac{y+1}{y-1}\right)^{1/2}e^{-iky}dy \quad (24)$$

$$\Delta F_4 = -\frac{2}{\pi}\int_1^{\infty}\left[\frac{df}{dy} - \frac{1}{ik}\frac{d^2f}{dy^2}\right][y-(y^2-1)^{1/2}]e^{-iky}dy \quad (25)$$

where y is a dummy variable of integration.

If the decay function has no singular points in quadrants III or IV of the complex plane then Eq. (15) yields

$$\Delta W = \sum_{n=1}^{\infty}e^{-kn\hat{h}}e^{ikns}\left[f(-ns-in\hat{h}) - 1 - \frac{1}{ik}\frac{df(-ns-in\hat{h})}{dy}\right] \quad (26)$$

The effect of these new terms, which are due to the decay function, is shown in Fig. 5. As may be seen in Fig. 4, the

wake sections directly below the rotor blade lose strength due to decay so that the wakes have less effect than they would if there were no decay. The result is that the decay function smooths out the variation of the lift deficiency function with respect to the reduced frequency. The wakes cause a lift loss and phase shift even at zero reduced frequency. With no decay,

$$C_1(0,\mu,\lambda) = \lambda - i\mu/(\lambda - i\mu + bc/2R)$$

For hover, this limit is the same as that found by Loewy[1] with zero frequency ratio.

Theodorsen Comparison

In Fig. 6 it is evident that there is a significant difference between the lift deficiency functions found from fixed wing theory (Theodorsen) and from forward flight helicopter theory as given here. This difference is especially noticeable at the low values of the reduced frequency where flutter will occur. Even with infinite inflow, a large difference exists between the values for the lift deficiency function found by fixed wing theory and the present theory due to the decay in the reference wake. If the vorticity strength is constant then $C_1(k,0,\hat{h}) = C'(k,M,\hat{h})$. That is, in hover the present theory reduces to that of Loewy with integer M frequency ratio. If, in addition, the wake spacing is made infinite then $C_1(k,0,\infty) = C(k)$ so that the present lift deficiency function reverts back to that of Theodorsen.

Unsteady Coefficients

For a thin airfoil experiencing harmonic bending-torsion oscillations, it can easily be shown that

$$\bar{v}_a(x) = iUk[h_0 + (x - a - i/k)\alpha_0] \tag{27}$$

Substituting Eq. (27) into Eq. (21) yields

$$L = -\pi\rho\omega^2c^3(L_Hh_0 + L_A\alpha_0) \tag{28}$$

where

$$L_H = L_h = 1 - 2iC_1(k,\mu,\lambda)/k \tag{29}$$

$$L_A = L_\alpha - (\tfrac{1}{2} + a)L_h \tag{30}$$

where

$$L_\alpha = \tfrac{1}{2} - i[1 + 2C_1(k,\mu,\lambda)]/k - 2C_1(k,\mu,\lambda)/k^2$$

and ac is the distance (positive aft) from the midchord to the elastic axis.

The moment about the elastic axis is

$$M_{ea} = c^2\int_{-1}^{1}\Delta p(x)(x - a)dx$$

So, use of Eq. (20) for $\Delta p(x)$ and Eq. (27) for $\bar{v}_a(x)$ yields

$$M_{ea} = \pi\rho\omega^2c^4(M_Hh_0 + M_A\alpha_0) \tag{31}$$

where

$$M_H = M_h - (\tfrac{1}{2} + a)L_h \tag{32}$$

$$M_A = M_\alpha - (\tfrac{1}{2} + a)(L_\alpha + M_h) + (\tfrac{1}{2} + a)^2L_h \tag{33}$$

where

$$M_h = \tfrac{1}{2} + M_D$$

and

$$M_\alpha = \tfrac{3}{8} - i/k + (2a + i/k)M_D$$

The term M_D appears due to the decay function and is given by

$$M_D = \frac{i}{k}\frac{\Delta F_2 + \frac{1}{2}\Delta F_5}{H_1^{(2)} + iH_0^{(2)} + \Delta F_3 + 2(W + \Delta W)(J_1 + iJ_0)} \tag{34}$$

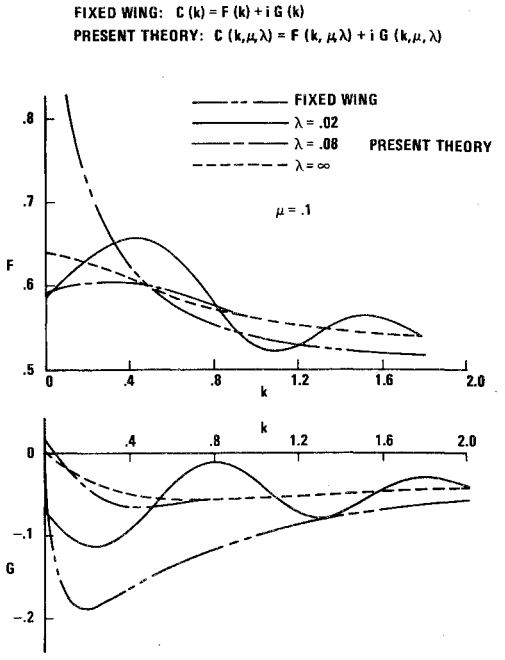

Fig. 6 Comparison of present theory with fixed wing (Theodorsen).

where

$$\Delta F_5 = -\frac{2}{\pi}\int_1^\infty y\left(\frac{df}{dy} - \frac{1}{ik}\frac{d^2f}{dy^2}\right)[y - (y^2 - 1)^{1/2}]e^{-iky}\,dy \tag{35}$$

With a damping coefficient of g the equations of motion for the blade section are

$$\ddot{h} + x_\alpha\ddot{\alpha} + \omega_h^2(1 + ig)h = -L/mc \tag{36}$$

$$x_\alpha\ddot{h} + r_\alpha^2\ddot{\alpha} + r_\alpha^2\omega_\alpha^2(1 + ig)\alpha = M_{ea}/mc^2 \tag{37}$$

where, $x_\alpha c$ is the distance between the center of gravity and the elastic axis, and $r_\alpha^2 = I_\alpha/mc^2$ = square of the radius of gyration.

The flutter determinant resulting from Eqs. (36) and (37) is

$$\begin{vmatrix}[Z - (\omega_\alpha/\omega_h)^2(1 + \kappa L_H)][-(\omega_\alpha/\omega_h)^2(x_\alpha + \kappa L_A)] \\ [-(x_\alpha + \kappa M_H/r_\alpha^2][Z - 1 - \kappa M_A/r_\alpha^2]\end{vmatrix} = 0 \tag{38}$$

where

$$Z = (\omega_\alpha/\omega)^2(1 + ig) \tag{39}$$

and

$$\kappa = \pi\rho^2c^2/m \tag{40}$$

For a given advance ratio, the reduced frequency can be varied in Eq. (38) until g passes through zero. This yields the flutter speed for this advance ratio from the relation

$$k_{FL} = \omega_{FL}c/V_{FL}$$

Results and Conclusions

Numerical Example

In order to explore trends resulting from this theory, the analysis was applied to a simplified numerical example, which considered bending-torsion flutter for the tip segment of a rotor blade. It should be noted that this is analogous to solving the wing flutter problem by only treating one section of a wing. Thus, for an actual analysis of an entire rotor blade, the blade should be treated as a number of segments

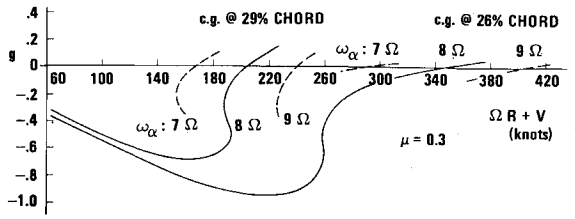

Fig. 7 Rotor blade V-g plot.

as would be done in the fixed-wing case. Since the blade inboard sections, if considered, would contribute positive damping to the blade, the results shown here will tend to exhibit lower flutter speeds than would be found in the actual case.

Characteristics of the blade considered are given in Table 1. Bending and torsion frequencies of 2.5Ω and 8Ω were selected so as to be representative of the first bending and torsion modes of a typical articulated rotor blade. Also, it was noted that variations in downwash could have a significant effect on results by causing wide variations in vertical spacing of wake layers. For the initial studies this parameter was held constant by setting induced velocity equal to a constant (80 in./sec) and keeping the rotor set at zero angle-of-attack at all airspeeds.

Trends Observed

Of interest is the $V - g$ type plot shown in Fig. 7 for the blade segment. Plotted is damping (g) required for neutral stability vs total airspeed ($\Omega R + V$). Plots are shown for the unstable mode (torsion) for three different c.g. locations. As would be expected, the flutter speed decreases as the c.g. is moved aft.

Figure 7 also shows the influence of torsional stiffness. If the torsional frequency was changed due to stiffness to say 7Ω or 9Ω, a new family of curves would result. Indicated on Fig. 7 are portions of these curves where they cross the flutter boundary. It can be seen that the flutter speed increases as torsional stiffness (frequency) increases.

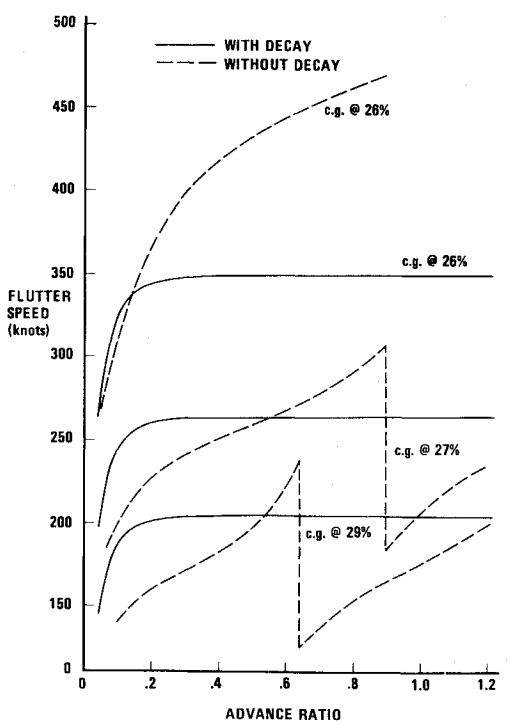

Fig. 8 Variation of flutter speed with advance ratio.

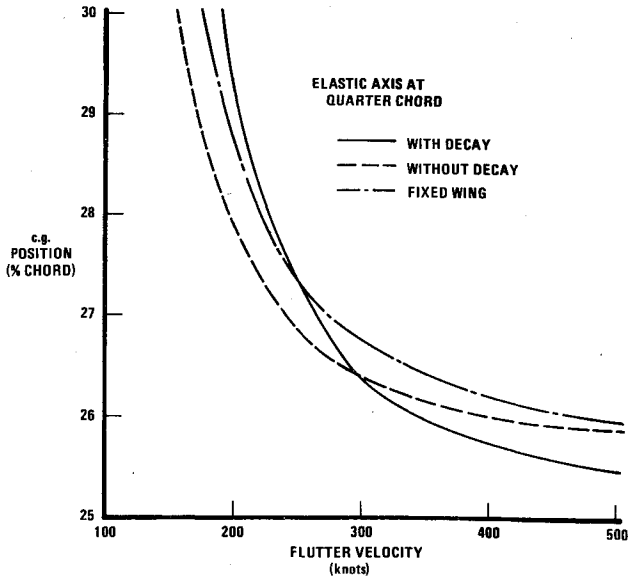

Fig. 9 Influence of c.g. position on blade segment flutter velocity.

Figure 8 depicts the influence on flutter speed of the build-up and decay of shed vorticity for several chordwise c.g. locations. We observe that with build-up and decay, changes in flutter speed due to advance ratio disappear for larger advance ratios. The flutter speed levels off because the distance between the blade and the center of strength for each shed wake increases with advance ratio. This increased separation can be seen from Fig. 4, and it reduces the effect that the wakes have on the flutter speed.

Also plotted in Fig. 8 is the case where no build-up and decay is introduced. Since the wakes, without this effect, extend infinitely forward and behind the rotor, the vorticity near the rotor will remain at full strength even at very high advance ratios. Thus the advance ratio will only affect phase, and so the flutter speed continues to change with advance ratio. The curves of Fig. 8 also confirm those of Fig. 7 in that flutter speed is seen to drop as the blade center of gravity is moved aft.

The relationship of 1) the present theory with build-up and decay of vorticity; 2) the present theory without this effect; and 3) quasi-fixed-wing flutter theory, is shown in Fig. 9. Plotted is blade segment c.g. position vs flutter speed ($\Omega R + V$) for a design advance ratio, $\mu = 0.3$. For the case shown there is a crossover of the curves. We observe when the blade c.g. is sufficiently removed from the elastic axis that fixed-wing flutter theory gives the most conservative results, whereas when the c.g. is near the quarter-chord the most conservative results are those given by the present theory.

Table 1 Characteristics of sample blade

Parameter	Value	Units
b	5	
m	0.46	lb/in.
I_α	1.97	lb in.
c	9.125	in.
R	31	ft
Ω	203	rpm
ρ	0.002378	lb sec²/ft⁴
v_i	80	in./sec
e.a.	25% chord	
ω_h	2.5Ω	
ω_α	8.0Ω	
x_{cg}	variable	

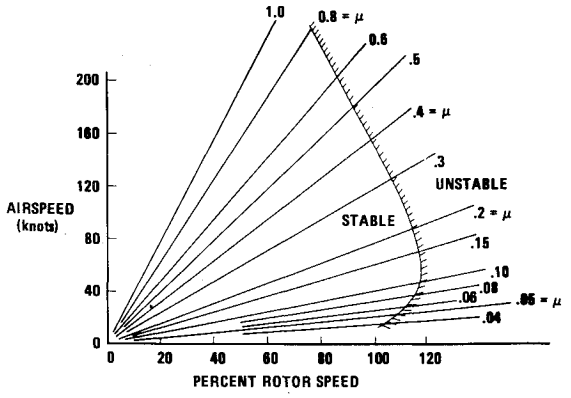

Fig. 10 Blade flutter boundary in terms of airspeed and rotor speed.

Application to Design

Results of a forward flight flutter analysis can be summarized in a design chart such as given by Fig. 10. Plotted is the airspeed of the aircraft vs percent rotor speed. Also indicated on the diagram are the blade flutter boundary and lines of constant advance ratio.

For example, for a compound helicopter in which rotor load and rotor speed can be reduced for higher advance ratios, the tip speed can be kept below the flutter speed by decreasing rotor speed as airspeed increases. The chart shows the safe operating region for the helicopter. With such a chart the pilot can readily determine what the maximum allowable rotor speed is for a given airspeed, or what airspeed can be attained with a given rotor speed. We observe from the plot that a rotor speed of 100% or less is required for an airspeed of 150 knots, and an airspeed of about 230 knots can be reached with a rotor speed of 80%. Other boundaries on the chart that might be used to bracket the flutter envelope are minimum and maximum rotor speed, and maximum advance ratio.

Observe the lower part of the flutter boundary curve in Fig. 10. This indicates that a reduction in rotor speed is required for the sample problem at low advance ratios. This is due to the grouping of rotor wakes at these low speeds. Within this region there would be a transition between the forward flight theory presented and that of Loewy.[1] Also, it can be seen that the flutter boundary curve shown in the figure becomes a straight line for advance ratios greater than $\mu = 0.25$. This is due to the effect previously noted that with higher advance ratio the more distant wakes have an increasingly smaller influence on the flutter speed.

Figure 10 is constructed by first drawing in the lines of constant advance ratio. Then, with the flutter speed determined for each advance ratio, the percent rotor speed is computed from, percent rotor speed = flutter speed/$\Omega R(1 + \mu)$. The point for this percent rotor speed is now marked on the appropriate advance ratio line, and connecting these points defines the flutter boundary.

Conclusions

To summarize the results of this paper, a lift deficiency function for a rotor blade in forward flight has been developed and related to that of Theodorsen[2] and Loewy.[1] It has been shown that the theory presented is consistent with their work for limiting conditions. For example, when forward flight speed is made to approach zero (hover) and the build-up and decay of the wakes is reduced to zero (constant-strength vorticity), then the lift-deficiency function becomes that of Loewy.[1] Further, if wake spacing below the rotor is made very large and constant-strength vorticity is maintained, then the theory can be shown to become that of Theodorsen[2] for the fixed-wing case.

Significant differences were noted between the lift deficiency function from fixed wing theory and that from the forward flight helicopter theory presented. These differences were especially noticeable at low values of reduced frequency where flutter generally occurs.

From the numerical example, several trends were noted that are typical of flutter theory in general. There was a reduction in flutter speed with rearward shift of blade center-of-gravity. Also, as blade torsional frequency was raised or lowered, there was a corresponding increase or decrease in blade flutter speed.

The build-up and decay of vorticity, that was inherent in the wake model, results in flutter speed becoming essentially constant when plotted with respect to advance ratio due to the reduced effect of the more distant wakes on the flutter speed at higher advanced ratios.

References

[1] Loewy, R. G., "A Two-Dimensional Approach to the Unsteady Aerodynamics of Rotary Wings," *Journal of the Aeronautical Sciences*, Vol. 24, Feb. 1957, pp. 82–98.

[2] Theodorsen, T., "General Theory of Aerodynamic Instability and the Mechanism of Flutter," Rept. 496, 1935, NACA.

[3] Schwarz, L., "Berechnung der Drückverteilung einer harmonisch sich Verformenden Tragflache in ebener Strömung," *Luftfahrtforschung*, Band 17, Nr. 11 and 12, Dec. 1940.

[4] Söhngen, H., "Die Lösungen der Integralgleichung und deren Anwendung in der Tragflugeltheorie," *Mathematische Zeitschrift*, Band 45, 1939, pp. 245–264.

[5] Jones, W. P., "Aerodynamic Forces on Wings in Non-uniform Motion," Repts. and Memo. 2117, British Aeronautical Research Council, 1945.

[6] Jones, W. P. and Rao, B. M., "Compressibility Effects on Oscillating Rotor Blades in Hovering Flight," *Volume of Technical Papers on Structural Dynamics and Aeroelasticity Specialist Conference*, New Orleans, La., April 16–17, 1969.

[7] Hammond, C. E., "Compressibility Effects in Helicopter Rotor Blade Flutter," Ph.D. thesis, Dec. 1969, Georgia Inst. of Technology.

[8] Jones, J. P., "The Influence of the Wake on the Flutter and Vibration of Rotor Blades," *The Aeronautical Quarterly*, Aug. 1958, pp. 258–286.

[9] Meyer, J. R. Jr., "An Investigation of Bending Moment Distribution on a Model Helicopter Blade," TN 2626, Feb. 1952, NACA.